

Mechanisms of Brønsted Acid Catalyzed Additions of Phenols and Protected Amines to Olefins: A DFT Study

Xin Li,^[a] Siyu Ye,^[a] Chuan He,^[b] and Zhi-Xiang Yu*^[a]

Keywords: Nucleophilic addition / Brønsted acids / Density functional calculations / Reaction mechanisms / Alkenes

DFT calculations at the B3LYP/6-31G(d) level were performed to understand the mechanism of the recently developed trifluoromethanesulfonic acid (TfOH) catalyzed intermolecular additions of phenols and protected amines to simple olefins. A novel mechanism involving a concerted, eight-membered-ring transition structure for the addition of the alcohol/amine to the alkene with TfOH as a catalyst was located. In the addition transition structure, the alkene sub-

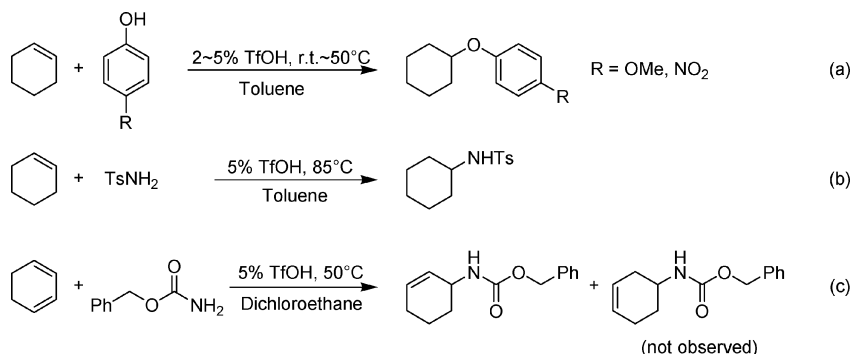
strate is protonated and has significant carbocation character. Calculations to rationalize the relative reactivities of the alcohols and amines, together with the regioselectivity of amide addition to the diene, were also conducted. Factors affecting isomerization of the alkene substrates in the alcohol addition process are discussed.

(© Wiley-VCH Verlag GmbH & Co. KGaA, 69451 Weinheim, Germany, 2008)

Introduction

Atom-economical nucleophilic additions of the hydroxy and amino groups of phenols, carboxylic acids, and protected amines to unsaturated C–C multiple bonds are important reactions used to form C–O and C–N bonds.^[1] Tremendous effort to achieve such transformations has been made by synthetic chemists. The commonly applied methods to achieve these additions are those using either transition-metal catalysts (such as Pd, Rh, Ru, Pt, Au complexes,

lanthanides, actinides) or main-group metal catalysts.^[2] In order to overcome the expensiveness and toxicity of transition-metal and main-group metal catalysts, Brønsted acids have been exploited to catalyze C–O and C–N bond-formation reactions.^[3] This exploration is mainly rooted in the facts that Brønsted acids can electrophilically activate C–C double bonds to promote the formation of the C–O and C–N bonds.



Scheme 1. TfOH-catalyzed addition of phenols and amides to alkenes.^[2k]

[a] Beijing National Laboratory for Molecular Sciences (BNLMS), Key Laboratory of Bioorganic Chemistry and Molecular Engineering of Ministry of Education, College of Chemistry, Peking University
Beijing 100871, P. R. China
Fax: +86-010-6275-2612
E-mail: yuzx@pku.edu.cn

[b] Department of Chemistry, The University of Chicago
5735 South Ellis Avenue, Chicago, Illinois 60637, USA
Supporting information for this article is available on the WWW under <http://www.eurjoc.org> or from the author.

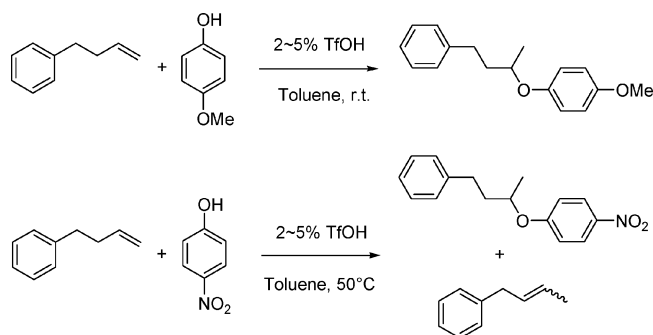
Brønsted acid catalyzed hydroamination was recently achieved by the Beller and Hartwig groups, respectively.^[4] Later, the Arnold and Bergman groups extended the acid-catalyzed hydroamination of activated alkenes with anilines to an intermolecular version.^[5] The intramolecular version of the addition of alcohols to alkenes has been well developed and has wide applications in organic synthesis. For example, the recent synthesis of platensimycin by Nicolaou

involves such a transformation.^[6,7] However, its intermolecular version has been rarely reported.

In 2006, He and coworkers demonstrated that trifluoromethanesulfonic acid (TfOH) can catalyze the intermolecular addition of phenols, carboxylic acids, and tosylamides to unactivated alkenes under relatively mild conditions,^[2k] as exemplified by the reactions shown in Scheme 1.

Although hydration of alkenes catalyzed by Brønsted acids has been studied in detail for over fifty years,^[8] the mechanistic details about the recently developed acid-catalyzed direct additions of O–H and N–H bonds to unsaturated C–C multiple bonds remain unclear. Here we wish to report our DFT studies of the mechanisms of these acid-catalyzed reactions (Scheme 1). Our calculations will detail these acid-catalyzed processes at the molecular level, together with energetics and structures of the intermediates and transition structures involved. In addition, an in-depth analysis of our calculations to rationalize the different reactivities between phenols and tosylamides in these additions to olefins (Scheme 1, reactions a and b) will be provided. Furthermore, our DFT studies will explore the origin of the experimentally observed regioselectivity of the addition of benzyl carbamate (CbzNH₂) to 1,3-cyclohexene (Scheme 1, reaction c), where the nitrogen atom is exclusively added to the internal carbon atom (rather than the terminal carbon atom) of the diene moiety.

In the Brønsted acid catalyzed additions of phenols to acyclic olefins, in addition to the C–O bond-formation reaction, an interesting C–C double-bond migration reaction was also observed (Scheme 2, 60% yield). The C–C double-bond migration occurs when the phenol contains a strong electron-withdrawing group, whereas this migration does not occur when phenol is substituted with an electron-donating group (Scheme 2, *p*-nitrophenol vs. *p*-methoxyphenol). Therefore, our computational study was also aimed to investigate the alkene isomerization mechanism and its energetic preference with respect to the addition process.



Scheme 2. TfOH-catalyzed phenol addition vs. alkene isomerization.^[2k]

The present mechanistic study will provide an in-depth understanding of the details of the acid-catalyzed C–O and C–N bond formations. The mechanistic insights could also be useful to understand other transition-metal-catalyzed reactions, which have been speculated to be catalyzed by

acids.^[9] The mechanistic information obtained can be used to guide the design of chiral Brønsted acids for asymmetric C–O and C–N bond-formation reactions and to help understand the recent asymmetric Brønsted acid catalyzed reactions in general.^[10]

Results and Discussion

We will first discuss the mechanism of Brønsted acid catalyzed intermolecular addition of phenol to olefins and the substituent effects in this reaction. A similar mechanism of addition of tosylamide to olefins will also be discussed. Then, we will investigate the regioselectivity in the hydroamination of 1,3-dienes. Finally, we will explore the terminal olefin migration process and explain why some additions are faster than the double-bond migration. The discussed relative energies in our work are B3LYP/6-31G(d)-computed Gibbs free energies in the gas phase, unless specifically noted.

The Mechanism of Brønsted Acid Catalyzed Addition of Phenol to Olefin and the Effect of Substituents

Figure 1 shows the computed energy surface for the TfOH-catalyzed addition of phenol to cyclohexene in the gas phase. The optimized structures involved in this addition are also given in Figure 1. In the first step of the addition reaction, cyclohexene, phenol, and TfOH are found to form complex **1**.^[11] This complexation process is exothermic by 12.6 kcal mol⁻¹, but it is endergonic by 5.9 kcal mol⁻¹, because of the entropy penalty for bringing three molecules together. Formation of stable complex **1** is mainly due to three favorable interactions between the reactants and catalyst. One stabilization interaction in complex **1** is the hydrogen-bonding interaction between the O8–H7 hydroxy group of the phenol and the O6 atom in the TfOH catalyst, as demonstrated by the nearly linear O8–H7···O6 geometry with a H7···O6 distance of 1.93 Å and a O8–H7···O6 angle of 164.7°. The other stabilization encountered in complex **1** comes from attraction between the C–C π bond in cyclohexene and the proton in TfOH. In complex **1**, the distances of C1···H3 and C2···H3 are 2.15 and 2.11 Å, respectively. This interaction resembles the protonation process of alkenes by strong acids.^[12] The third stabilization in complex **1** is the C1–H9···O8 interaction. The H9···O8 distance here is 2.47 Å, shorter than the sum of the van der Waals radius of hydrogen and oxygen. Such C–H···O interactions can be found in many organic and biological systems.^[13] In addition, there exists a relatively weak C–H···F interaction in complex **1**, which involves C2–H10···F11 interaction between cyclohexene and the CF₃ group of the catalyst. Both the C1–H9 and C2–H10 distances in complex **1** are 1.09 Å.

We computed the bond critical points (BCPs) in complex **1** by using the atoms in molecules (AIM) theory^[14] to further explore the stabilization of C–H···X (X = O, F) interactions. Table 1 summarizes the computed electron density

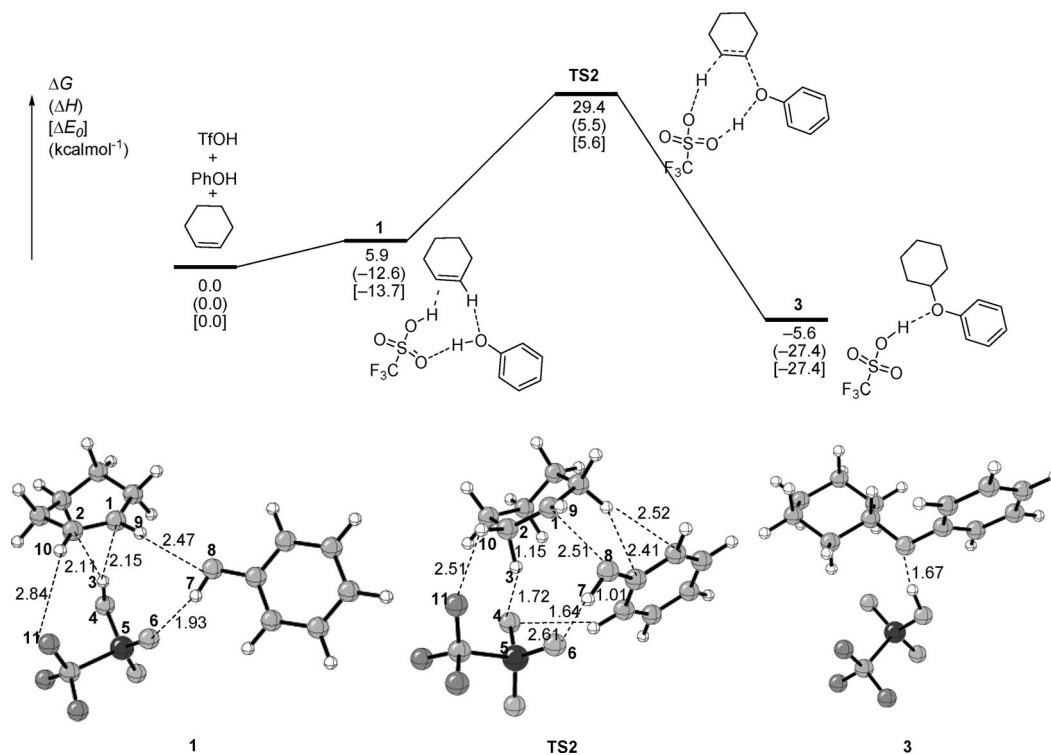


Figure 1. Reaction energy profile and optimized geometries of the TfOH-catalyzed addition of phenol to an olefin. Distances are in Å.

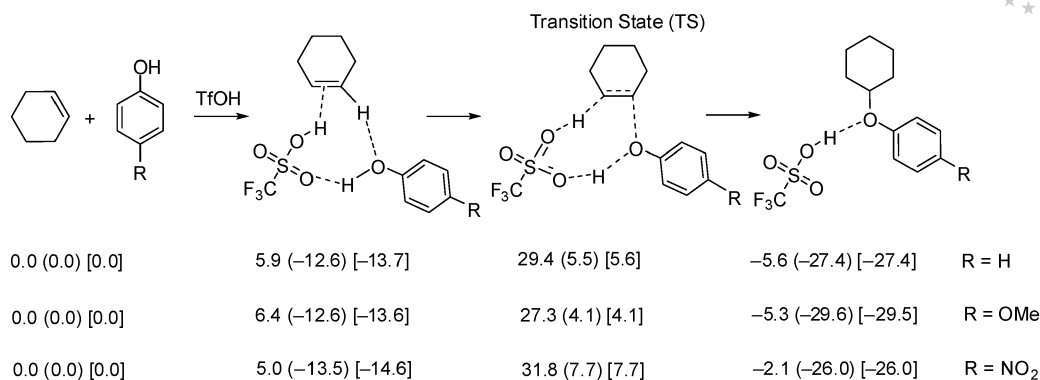
values (ρ_b), their Laplacian values ($\Delta^2\rho_b$, diagonalization of the Hessian of the electron density yields three eigenvalues, $\lambda_1 < \lambda_2 < \lambda_3$, and thus, $\Delta^2\rho_b = \lambda_1 + \lambda_2 + \lambda_3$), and the bond ellipticities ($\varepsilon = \lambda_1/\lambda_2 - 1$, measuring the extent to which charge is preferentially accumulated). If the computed electron density value is in the range of 0.002–0.035 au and its Laplacian value is in the range of 0.024–0.139 au,^[15] the corresponding interaction can be regarded as a strong interaction. The O8–H7...O6, $\pi(\text{C1}=\text{C2})\cdots\text{H3}-\text{O4}$, and C1–H9...O8 interactions have the computed electron density values of 0.0253, 0.0273, and 0.0095 au, respectively. Their Laplacian values are 0.0841, 0.0621, and 0.0335 au, respectively. Therefore, these three interactions can be regarded as strong interactions responsible for the stabilization of complex **1**.^[16] However, the C2–H10...F11 interaction has the computed electron density value of 0.0033 au and a Laplacian value of 0.0169 au. Therefore, this interaction is considered to be weak.

The addition reaction from complex **1** gives final complex **3** via concerted eight-membered-ring transition state **TS2**. The intrinsic reaction coordinate (IRC) calculation demonstrates that **TS2** directly connects complex **1** and complex **3** without involving the formation of any other intermediate. In **TS2**, the C2–H3 and C1–O8 bonds are forming and H7 is transferring from the hydroxy group of phenol to the O6 atom of TfOH. Because of this concerted character, the addition leads to the *cis* addition product. The total activation free energy^[17] is 29.4 kcal mol⁻¹, and the formation of complex **3** is exergonic by 5.6 kcal mol⁻¹, suggesting that this addition is feasible and does not require a high temperature. This is consistent with the experimental

Table 1. Analysis of several important bond critical points (BCPs) in complex **1**.

BCP	ρ_b	$\Delta^2\rho_b$	λ_1	λ_2	λ_3	ε
1	0.0253	0.0841	-0.0355	-0.0344	0.1540	0.0320
2	0.0273	0.0621	-0.0343	-0.0189	0.1153	0.8148
3	0.0095	0.0335	-0.0099	-0.0089	0.0523	0.1124
4	0.0033	0.0169	-0.0031	-0.0020	0.0220	0.5500

observation that the addition takes place at room temperature to 50 °C. Calculations in toluene solution also unveiled a concerted nature of this addition process (details in the Supporting Information). The calculated implicit solvation effect can roughly stabilize the separated reactants by 4.7 kcal mol⁻¹, but destabilize complex **1** and **TS2** by 3.7 and 0.9 kcal mol⁻¹, respectively. In addition, stepwise addition to generate carbocation intermediate is not favored energetically (endogonic by 62.1 kcal mol⁻¹ in solution). The recent theoretical study by the Goddard group also supported the concerted mechanism for the TsOH-cata-



Scheme 3. Computed relative energies (ΔG , ΔH in parentheses and ΔE_0 in square brackets, kcal mol⁻¹) for the TfOH-catalyzed addition of phenols to an olefin.

lyzed substitution, rather than the stepwise cationic mechanism.^[18d] The stepwise protonation/nucleophilic addition could be achieved when a superacid is used.^[2j]

Concerted **TS2** has an asynchronous character. In **TS2**, the forming C2–H3 bond length is 1.15 Å, which is very close to a normal C–H bond, implying that the protonation occurs prior to both the C1–O8 bond formation and the H7 shift process from O8 to O6. IRC calculations also demonstrate that the protonation of cyclohexene, the C1–O8 bond formation, and the H7 shift process from O8 to O6 take place in sequence. Therefore, in **TS2**, the cyclohexene moiety can be regarded as to have significant protonated character. Calculations show that the protonated cyclohexene in **TS2** has a positive charge of 0.701 electrons. Thus, it is expected that any factor that can stabilize the positive charge at the protonated cyclohexene moiety of **TS2**, such as an electron-donating group nearby, can stabilize the transition state, and consequently, lower the activation barrier of the addition reaction.

We performed further calculations to investigate how various substituents in the phenols affect the reaction rates (Scheme 3). The computational results show that an electron-donating substituent on phenol enhances the addition, whereas an electron-withdrawing group reduces the reaction rate. For example, the activation free energy of TfOH-catalyzed addition of *p*-methoxyphenol to cyclohexene is 2.1 kcal mol⁻¹ lower than that of the addition of unsubstituted phenol, whereas the activation free energy of *p*-nitrophenol added to cyclohexene is 2.4 kcal mol⁻¹ higher. These computational results indicate that the reaction conditions can be milder when *p*-methoxyphenol is used as a substrate, consistent with the experimental observations.

The Mechanism of Brønsted Acid Catalyzed Addition of Tosylamide to an Olefin

The addition of tosylamide to cyclohexene shares the same concerted mechanism as that of phenol. The computational potential energy surface and the optimized structures of the stationary points are shown in Figure 2. Transition state **TS5** is also asynchronous because protonation of cyclohexene occurs prior to both C1–N2 bond formation

and proton transfer from N2 to O3 in the concerted process. The total activation free energy of the addition of tosylamide to cyclohexene is 35.8 kcal mol⁻¹, which is 6.4 kcal mol⁻¹ higher than that of the phenol addition. This is consistent with the experimental observation that tosylamide addition to inert olefins requires a higher reaction temperature than that of the phenol addition (Scheme 1).

The Hydroamination of a 1,3-Diene and Its Regioselectivity Catalyzed by a Brønsted Acid

TfOH-catalyzed hydroamination of CbzNH₂ to cyclohexadiene may occur at the internal or terminal carbon atom of the dienyl moiety to give two regioisomers. However, it is observed that the NHCbz group adds only towards the internal carbon atom of the dienyl moiety (Scheme 1, reaction c). To understand this regioselectivity better, we computed the potential energy surfaces for the addition of CbzNH₂ to the internal carbon atom (pathway 1) and to the terminal carbon atom (pathway 2) of the dienyl moiety in cyclohexadiene (Figure 3). The 1,4-addition of CbzNH₂ to cyclohexadiene may also give the experimentally obtained product, but we could not locate such a transition state. This is due to the formation of stable complexes **7** and **10**, which prefer to undergo 1,2-addition rather than 1,4-addition according to the principle of least motion of atoms.

Pathway 1 starts from formation of complex **7** among the olefin moiety, the catalyst, and the nucleophile. The nitrogen atom of the nucleophile is close to the internal carbon atom of the diene moiety. The complexation is exothermic by 12.1 kcal mol⁻¹. Then, through concerted but asynchronous transition state **TS8**, complex **7** is transformed into complex **9**, in which there is a hydrogen bond between the final addition product and the TfOH catalyst. The activation free energy of pathway 1 is 27.1 kcal mol⁻¹. Pathway 2 of nitrogen addition to the terminal carbon atom of the diene moiety shares a similar mechanism to that of pathway 1. The activation free energy of pathway 2 is 37.4 kcal mol⁻¹, which is 10.3 kcal mol⁻¹ higher than that of pathway 1, suggesting that only the internal addition product can be obtained, in agreement with the experimental

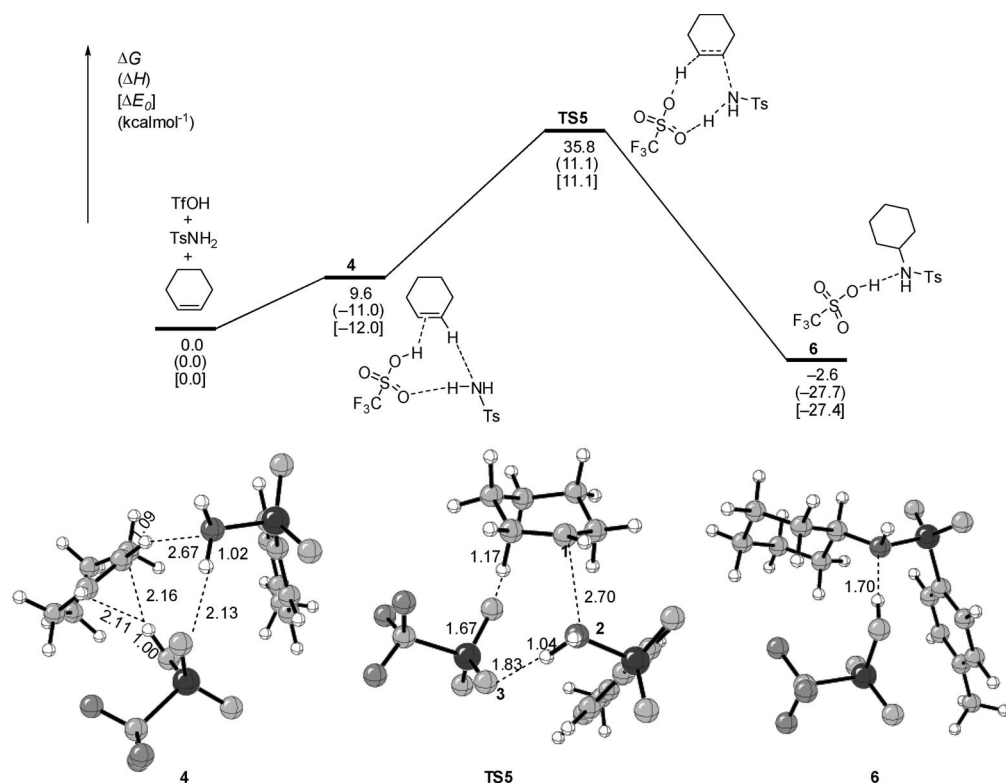


Figure 2. Potential energy profile of TfOH-catalyzed addition of tosylamide to an olefin. Distances are in Å.

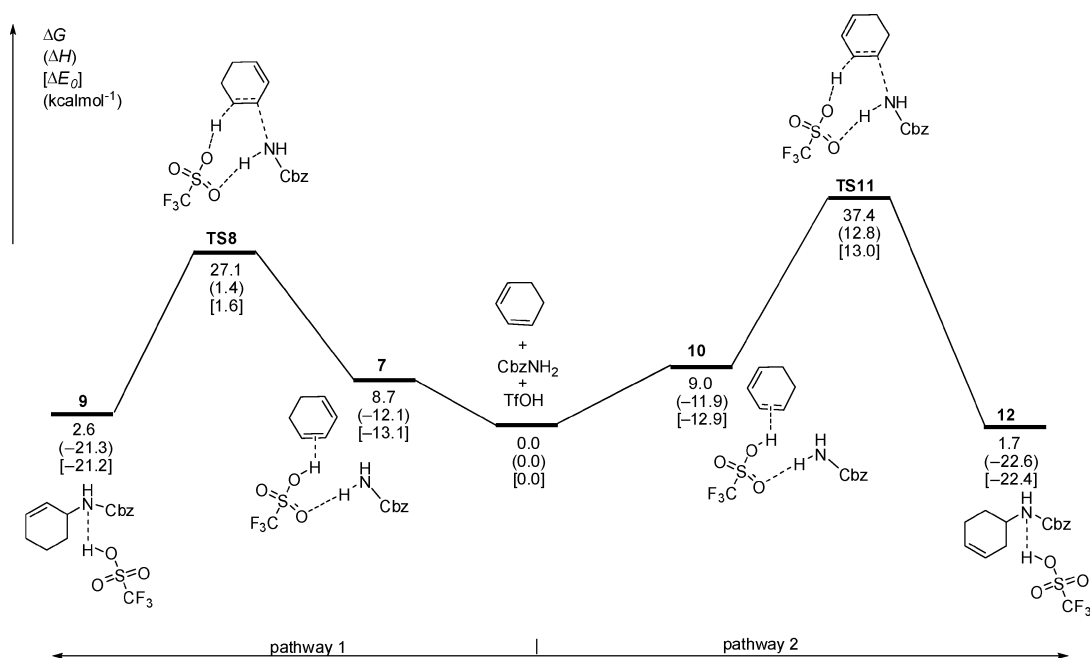


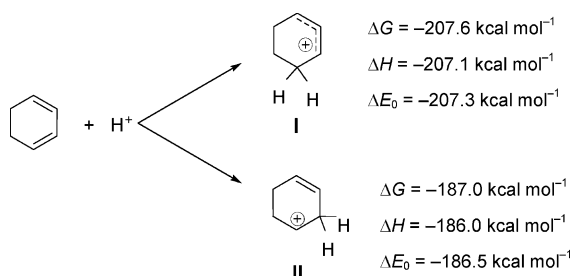
Figure 3. Potential energy profile of TfOH-catalyzed hydroamination of 1,3-cyclohexadiene.

results (Scheme 1, reaction c). This preference is even higher in dichloroethane solution, as the reaction barrier of pathway 1 is 14.3 kcal mol⁻¹ lower than that of pathway 2.

The preference for pathway 1 over pathway 2 can be understood by comparing the relative stabilities of **TS8** and **TS11**. Because the diene moieties in **TS8** and **TS11** are highly protonated, similar to **TS2** and **TS5** discussed above,

we can appreciate their relative stability by considering two protonated cyclohexadiene cations (Scheme 4).^[18] The terminal protonated cyclohexadiene **I**, similar to the cationic part in **TS8**, is an allylic carbocation; in contrast, the internal protonated cyclohexadiene **II**, similar to the cationic part in **TS11**, is an isolated carbocation. An allylic carbocation is more stable than an isolated carbocation because

of conjugation effects. Scheme 4 shows that the formation of an allylic carbocation is more exergonic than that of an isolated carbocation by $20.6 \text{ kcal mol}^{-1}$. Consequently, it is reasonable to understand why **TS8** with an allylic carbocation is more stable than **TS11** with an isolated carbocation. Therefore the exclusive regioselectivity of addition to cyclohexadiene can be well expected.



Scheme 4. Energies of protonation of cyclohexadiene.

Phenol Addition to Terminal Olefins: Addition Versus Double-Bond Migration

To rationalize why the double-bond migration can compete with the addition reaction of *p*-nitrophenol to an acyclic olefin (Scheme 2), the activation free energies of the additions of *p*-methoxyphenol and *p*-nitrophenol must be compared with that of the double-bond migration reaction. The computational energy surfaces of additions of *p*-methoxyphenol and *p*-nitrophenol to an alkene are shown in Figure 4, where we used 1-pentene as a model for the experimentally used acyclic olefin.

Phenol addition to the olefin prefers to add to the internal carbon atom of 1-pentene, following the Markonikov rule for the addition of acids to alkenes.^[19] This addition

selectivity can be rationalized by the fact that the addition of phenol to the internal carbon atom is through a transition state with secondary carbocation character, whereas the alternative addition is through a transition state with primary carbocation character. The activation free energy of *p*-methoxyphenol addition is $25.3 \text{ kcal mol}^{-1}$, whereas that of *p*-nitrophenol is $27.3 \text{ kcal mol}^{-1}$. This suggests that the former addition is faster than the latter [B3LYP/6-311++G(d,p) single-point calculations also show that the difference in the activation barrier is about $2.5 \text{ kcal mol}^{-1}$ in terms of electronic energy]. Both addition reactions have their respective competitive double-bond isomerizations, as discussed below.

Figure 5 shows the energy surface of the TfOH-catalyzed isomerization of alkenes. Isomerization can lead to either *cis*- or *trans*-alkenes via concerted transition states. Calculations indicate that the formation of a *cis*-alkene is slightly favored over that of a *trans*-alkene (26.8 vs. $27.5 \text{ kcal mol}^{-1}$ in terms of activation free energy). The activation free energies of both isomerization processes are higher than that of the *p*-methoxyphenol addition by 1.5 and $2.2 \text{ kcal mol}^{-1}$, respectively. This suggests that the *p*-methoxyphenol addition is faster than the double-bond isomerization, so the isomerization may not be observed experimentally. However, alkene isomerization competes with addition in the *p*-nitrophenol case because both processes have very close activation free energies ($26.8 \text{ kcal mol}^{-1}$ for isomerization vs. $27.3 \text{ kcal mol}^{-1}$ for addition reaction). Consequently, the addition of electron-deficient phenols to alkenes will be accompanied by the double-bond isomerization, whereas the alkene isomerization is not favored when electron-rich phenols are used. In the latter case, formation of the addition products is dominant. The present calculations agree with the experimental findings quite well. These calculations also

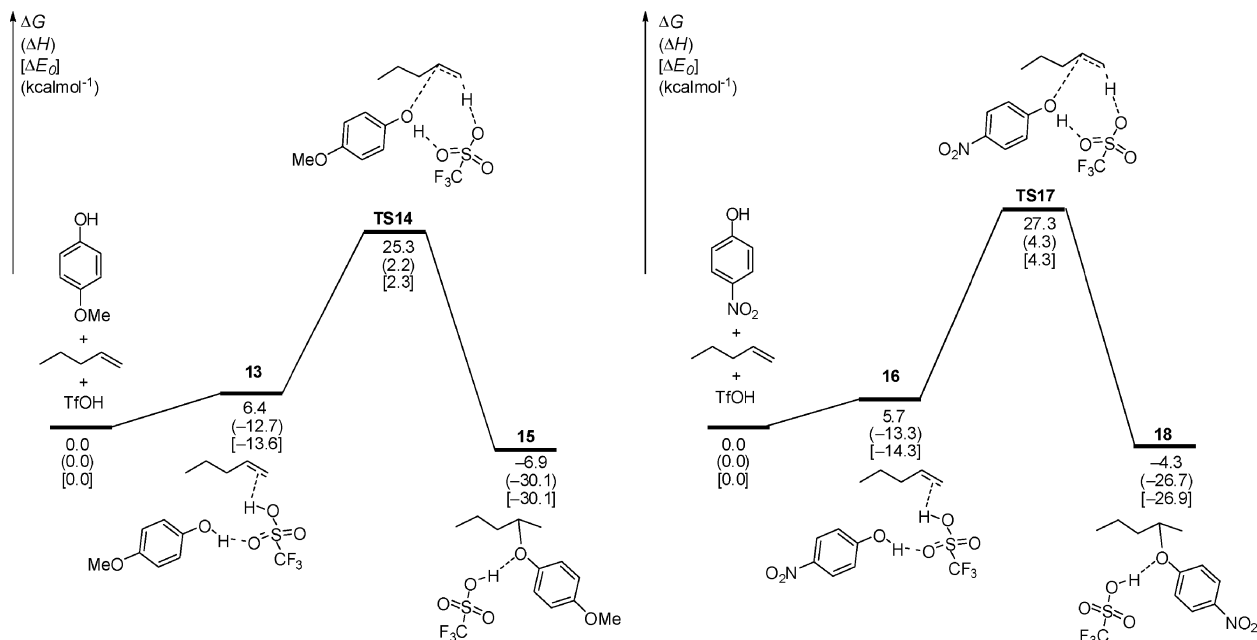


Figure 4. Potential energy profiles of TfOH-catalyzed intermolecular addition of *p*-methoxyphenol (left) and *p*-nitrophenol (right) to a terminal olefin.

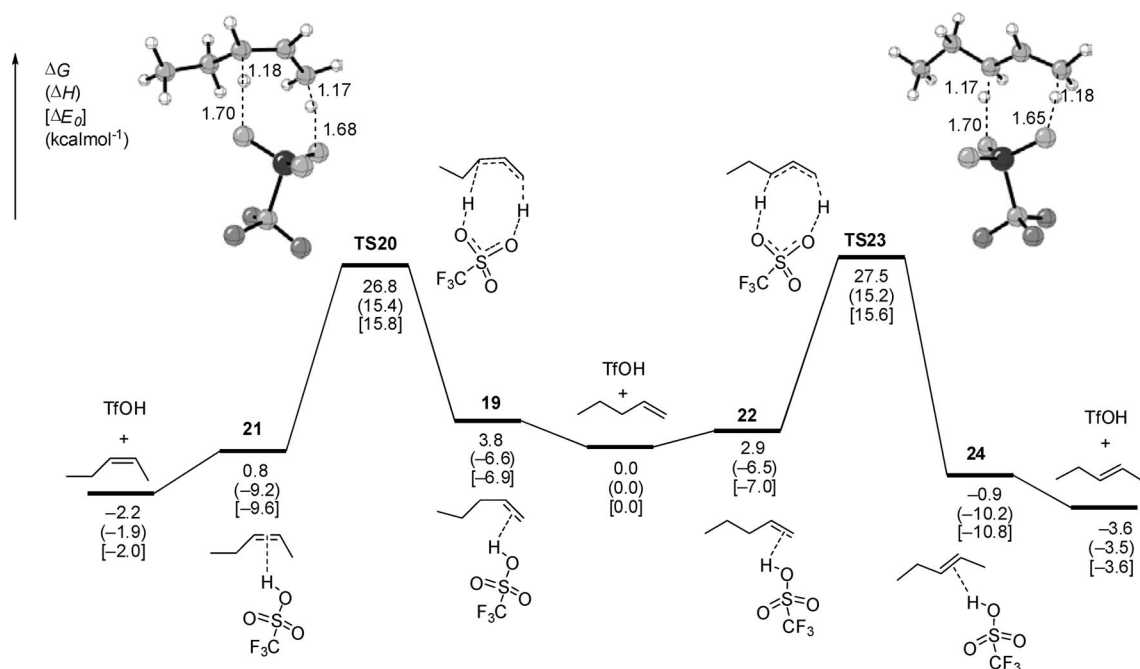


Figure 5. Potential energy profile of TfOH-mediated terminal olefin migration.

suggest that isomerization of the alkenes can be avoided if phenols bearing electron-donating substitutions are employed in the addition reaction.

Conclusions

The mechanisms of Brønsted acid catalysis are important and fundamental for understanding classic reactions in organic synthesis. In the present investigation, we studied TfOH-catalyzed intermolecular additions of phenols and protected amines to olefins and 1,3-dienes with the aid of density functional theory calculations. The activation by TfOH brings the nucleophilic addition to work through a concerted eight-membered-ring transition state, which is highly asynchronous with the alkene substrate significantly protonated. Different substituents on the phenol can increase or decrease the activity of the substrate. The addition of tosylamide to an unactivated olefin possesses a high activation energy relative to that of phenols to olefins, although their reaction mechanisms are similar. For the hydroamination of 1,3-dienes, the amine prefers to add to the internal carbon atom of the diene moiety. Double-bond migration of the alkenes is a competitive process with respect to the addition process. The extent of these two competitive processes depends on the relative reactivities of the phenols used.

Computational Methods

All calculations were carried out with DFT method^[20] as implemented in GAUSSIAN 03.^[21] All structures were optimized by the B3LYP/6-31G(d) method. Additional calculations with basis sets containing diffuse functions at the B3LYP/6-31+G(d) and

B3LYP/6-311++G(d,p)//B3LYP/6-31G(d) levels have also been performed for the reaction shown in Figure 1. These additional calculations gave similar relative energies as those obtained by the B3LYP/6-31G(d) method, suggesting that B3LYP/6-31G(d) is appropriate to study the TfOH-catalyzed additions in this paper (see Table S2 in the Supporting Information). The stationary points were characterized by harmonic analysis. For all the transition structures, the vibration related to the imaginary frequency corresponds to the nuclear motion along the reaction coordinate. Intrinsic reaction coordinate (IRC)^[22] calculations were performed to ensure that the transition structures connect related intermediates correctly. Unless specifically mentioned, the discussed Gibbs free energy (ΔG), the enthalpy (ΔH), and the zero-point corrected energy (ΔE_0) were computed at 298 K in the gas phase by using the B3LYP/6-31G(d) method. The solvation energies for certain important structures were calculated by single-point calculations on the optimized structures with the polarized continuum model (PCM)^[23] by using UAHF radii. The natural charges were calculated by natural population analysis (NPA)^[24] at the same theoretical level as that used for geometry optimization. Topological analysis of electron densities at bond critical points was performed with the AIM 2000 program.^[25]

Supporting Information (see footnote on the first page of this article): Complexes of TfOH, alkene and phenol; comparison of the intermolecular addition of phenol to olefin catalyzed by TfOH and its $C(\text{CH}_3)_3\text{SO}_3\text{H}$ analog; regioselectivity of the addition of *p*-methoxyphenol to the terminal olefin; energy differences between precursor complexes and transition states in the gas phase and in solution; discussions of possible stepwise mechanism of addition in solution; effects of basis sets; cartesian coordinates and energies of all species.

Acknowledgments

We are grateful for generous financial support from the Excellent Researches in Peking University (985 Program), the Natural Sci-

ence Foundation of China (20772007 and 20672005), and the Scientific Research Foundation for the Returned Overseas Chinese Scholars, State Education Ministry of China.

- [1] a) V. Baliah, R. Jeyaraman, L. Chandrasekaran, *Chem. Rev.* **1983**, *83*, 379; b) R. R. Schmidt, *Acc. Chem. Res.* **1986**, *19*, 250; c) T. E. Müller, M. Beller, *Chem. Rev.* **1998**, *98*, 675; d) M. Beller, J. Seayad, A. Tillack, H. Jiao, *Angew. Chem. Int. Ed.* **2004**, *43*, 3368; e) S. Hong, T. J. Marks, *Acc. Chem. Res.* **2004**, *37*, 673; f) A. Deiters, S. F. Martin, *Chem. Rev.* **2004**, *104*, 2199.
- [2] For selected recent reports, see: a) A. Takemiya, J. F. Hartwig, *J. Am. Chem. Soc.* **2006**, *128*, 6042; b) S. B. Herzon, J. F. Hartwig, *J. Am. Chem. Soc.* **2007**, *129*, 6690; c) Y. Oe, T. Ohta, Y. Ito, *Chem. Commun.* **2004**, 1620; d) J. A. Bexrud, J. D. Beard, D. C. Leitch, L. L. Schafer, *Org. Lett.* **2005**, *7*, 1959; e) M. R. Crimmin, I. J. Casely, M. S. Hill, *J. Am. Chem. Soc.* **2005**, *127*, 2042; f) C. F. Bender, R. A. Widenhofer, *J. Am. Chem. Soc.* **2005**, *127*, 1070; g) J. Zhang, C.-G. Yang, C. He, *J. Am. Chem. Soc.* **2006**, *128*, 1798; h) X. Zhang, A. Corma, *Chem. Commun.* **2007**, 3080; i) J. Michaux, V. Terrasson, S. Marque, J. Wehbe, D. Prim, J.-M. Campagne, *Eur. J. Org. Chem.* **2007**, 2601; j) G. A. Olah, *Angew. Chem. Int. Ed. Engl.* **1995**, *34*, 1393; k) Z. Li, J. Zhang, C. Brouwer, C.-G. Yang, N. W. Reich, C. He, *Org. Lett.* **2006**, *8*, 4175, and references cited therein; l) K. Komeyama, T. Morimoto, K. Takaki, *Angew. Chem. Int. Ed.* **2006**, *45*, 2938; for a recent review on gold chemistry and the chemistry of gold-catalyzed nucleophilic additions, see: m) A. S. K. Hashmi, G. J. Hutchings, *Angew. Chem. Int. Ed.* **2006**, *45*, 7896.
- [3] Base-catalyzed hydroamination is also developed, see a review: J. Seayad, A. Tillack, C. G. Hartung, M. Beller, *Adv. Synth. Catal.* **2002**, *344*, 795.
- [4] a) M. Beller, O. R. Thiel, H. Trauthwein, *Synlett* **1999**, 243; b) B. Schlummer, J. F. Hartwig, *Org. Lett.* **2002**, *4*, 1471.
- [5] L. L. Anderson, J. Arnold, R. G. Bergman, *J. Am. Chem. Soc.* **2005**, *127*, 14542.
- [6] a) K. C. Nicolaou, A. Li, D. J. Edmonds, *Angew. Chem. Int. Ed.* **2006**, *45*, 7086.
- [7] For selected other references, see: a) Q. Wang, Q. Huang, B. Chen, J. Lu, H. Wang, X. She, X. Pan, *Angew. Chem. Int. Ed.* **2006**, *45*, 3651; b) R. Heim, S. Wiedemann, C. M. Williams, P. V. Bernhardt, *Org. Lett.* **2005**, *7*, 1327.
- [8] a) J. B. Levy, R. W. Taft, L. P. Hammett, *J. Am. Chem. Soc.* **1953**, *75*, 1253; b) A. V. Willi, *Helv. Chim. Acta* **1964**, *47*, 647; c) A. V. Willi, *Helv. Chim. Acta* **1964**, *47*, 655; d) G. Modena, F. Rivetti, G. Scorrano, U. Tonellato, *J. Am. Chem. Soc.* **1977**, *99*, 3392.
- [9] P. N. Liu, Z. Y. Zhou, C. P. Lau, *Chem. Eur. J.* **2007**, *13*, 8610.
- [10] After submission of this paper, Ackermann and Althammer reported that phosphoric acid can catalyze the intramolecular addition of amines to alkenes. This reaction has been developed to an asymmetric one with low stereoselectivity. For details, see: a) L. Ackermann, A. Althammer, *Synlett* **2008**, 995. For recent reviews on phosphoric acids as catalysts, see: b) T. Akiyama, J. Itoh, K. Fuchibe, *Adv. Synth. Catal.* **2006**, *348*, 999; for pioneering works, see: c) D. Uraguchi, M. Terada, *J. Am. Chem. Soc.* **2004**, *126*, 5356; d) T. Akiyama, J. Itoh, K. Yokota, K. Fuchibe, *Angew. Chem. Int. Ed.* **2004**, *43*, 1566; for recent other examples, see: e) J. Seayad, A. M. Seayad, B. List, *J. Am. Chem. Soc.* **2006**, *128*, 1086; f) Y.-X. Jia, J. Zhong, S.-F. Zhu, C.-M. Zhang, Q.-L. Zhou, *Angew. Chem. Int. Ed.* **2007**, *46*, 5565; g) Q.-X. Guo, H. Liu, C. Guo, S.-W. Luo, Y. Gu, L.-Z. Gong, *J. Am. Chem. Soc.* **2007**, *129*, 3790, and references therein.
- [11] TfOH can coordinate the olefin to form complex **1'**, which is also a relatively stable species in the system, but the phenol can further form a hydrogen bond with **1'**, leading to the formation of true reactive intermediate **1**. See the Supporting Information for details.
- [12] For a review on addition reactions, see: F. A. Carroll, *Perspectives on Structure and Mechanism in Organic Chemistry*, Brooks/Cole Publishing Company, **1998**.
- [13] For experimental and computational studies on C–H···O interactions, see: a) I. Washington, K. N. Houk, *Angew. Chem. Int. Ed.* **2001**, *40*, 4485; b) F. M. Raymo, M. D. Bartberger, K. N. Houk, J. F. Stoddart, *J. Am. Chem. Soc.* **2001**, *123*, 9264; c) E. Arbely, I. T. Arkin, *J. Am. Chem. Soc.* **2004**, *126*, 5362; d) H. Matsuura, H. Yoshida, M. Hieda, S.-y. Yamanaka, T. Harada, K. Shin-ya, K. Ohno, *J. Am. Chem. Soc.* **2003**, *125*, 13910; e) R. Vargas, J. Garza, D. A. Dixon, B. P. Hay, *J. Am. Chem. Soc.* **2000**, *122*, 4750; f) S. Scheiner, T. Kar, Y. Gu, *J. Biol. Chem.* **2001**, *276*, 9832.
- [14] U. Koch, P. L. A. Popelier, *J. Phys. Chem.* **1995**, *99*, 9747.
- [15] P. L. A. Popelier, *J. Phys. Chem. A* **1998**, *102*, 1873.
- [16] For discussions on hydrogen-bond interactions, see: a) L. González, O. Mó, M. Yáñez, *J. Phys. Chem. A* **1997**, *101*, 9710; b) L. González, O. Mó, M. Yáñez, *J. Comput. Chem.* **1997**, *18*, 1124.
- [17] When the TfOH catalyst is replaced by (CH₃)₃CSO₃H, the activation energy of the addition increases by 3.3 kcal mol⁻¹. Details are given in the Supporting Information.
- [18] For recent theoretical studies on protonation and carbocations, see: a) P. Gutta, D. J. Tantillo, *Org. Lett.* **2007**, *9*, 1069; b) R. Ponec, P. Bultinck, P. Gutta, D. J. Tantillo, *J. Phys. Chem. A* **2006**, *110*, 3785; c) P. Gutta, D. J. Tantillo, *J. Am. Chem. Soc.* **2006**, *128*, 6172; d) M. Jacobsson, J. Oxgaard, C.-O. Abrahamsson, P.-O. Norrby, W. A. Goddard III, U. Ellervik, *Chem. Eur. J.* **2008**, *14*, 3954.
- [19] For the addition of phenol to the terminal olefin, the favored reaction pathway is addition to the internal carbon atom and not the terminal carbon atom of the alkene. See the Supporting Information for details.
- [20] a) A. D. Becke, *J. Chem. Phys.* **1993**, *98*, 5648; b) C. Lee, W. Yang, R. G. Parr, *Phys. Rev. B* **1988**, *37*, 785.
- [21] M. J. Frisch, G. W. Trucks, H. B. Schlegel, G. E. Scuseria, M. A. Robb, J. R. Cheeseman, J. A. Montgomery Jr., T. Vreven, K. N. Kudin, J. C. Burant, J. M. Millam, S. S. Iyengar, J. Tomasi, V. Barone, B. Mennucci, M. Cossi, G. Scalmani, N. Rega, G. A. Petersson, H. Nakatsuji, M. Hada, M. Ehara, K. Toyota, R. Fukuda, J. Hasegawa, M. Ishida, T. Nakajima, Y. Honda, O. Kitao, H. Nakai, M. Klene, X. Li, J. E. Knox, H. P. Hratchian, J. B. Cross, C. Adamo, J. Jaramillo, R. Gomperts, R. E. Stratmann, O. Yazyev, A. J. Austin, R. Cammi, C. Pomelli, J. W. Ochterski, P. Y. Ayala, K. Morokuma, G. A. Voth, P. Salvador, J. J. Dannenberg, V. G. Zakrzewski, S. Dapprich, A. D. Daniels, M. C. Strain, O. Farkas, D. K. Malick, A. D. Rabuck, K. Raghavachari, J. B. Foresman, J. V. Ortiz, Q. Cui, A. G. Baboul, S. Clifford, J. Cioslowski, B. B. Stefanov, G. Liu, A. Liashenko, P. Piskorz, I. Komaromi, R. L. Martin, D. J. Fox, T. Keith, M. A. Al-Laham, C. Y. Peng, A. Nanayakkara, M. Challacombe, P. M. W. Gill, B. Johnson, W. Chen, M. W. Wong, C. Gonzalez, J. A. Pople, *Gaussian 03*, Revision C.02, Gaussian, Inc., Wallingford CT, **2004**.
- [22] a) K. Fukui, *J. Phys. Chem.* **1970**, *74*, 4161; b) K. Fukui, *Acc. Chem. Res.* **1981**, *14*, 363; c) C. Gonzalez, H. B. Schlegel, *J. Phys. Chem.* **1990**, *94*, 5523.
- [23] a) M. Cossi, G. Scalmani, N. Rega, V. Barone, *J. Chem. Phys.* **2002**, *117*, 43; b) J. Tomasi, B. Mennucci, R. Cammi, *Chem. Rev.* **2005**, *105*, 2999.
- [24] a) A. E. Reed, R. B. Weinstock, F. Weinhold, *J. Chem. Phys.* **1985**, *83*, 735; b) A. E. Reed, L. A. Curtiss, F. Weinhold, *Chem. Rev.* **1988**, *88*, 899.
- [25] a) R. F. W. Bader, *Atoms in Molecules. A Quantum Theory*, Clarendon, Oxford, **1990**; b) F. Biegler-König, J. Schönbohm, D. Bayles, *J. Comput. Chem.* **2001**, *22*, 545; c) F. Biegler-König, J. Schönbohm, *J. Comput. Chem.* **2002**, *23*, 1489.

Received: April 2, 2008

Published Online: July 9, 2008